Wahono *et al.*
Egyptian Journal of Medical Human Genetics (2024) 25:52
https://doi.org/10.1186/s43042-024-00510-9

Egyptian Journal of Medical Human Genetics

RESEARCH

Open Access

Exploring the potential of phytoconstituents from *Phaseolus vulgaris* L against C-X-C motif chemokine receptor 4 (CXCR4): a bioinformatic and molecular dynamic simulations approach

Cesarius Singgih Wahono[1,2], Mokhamad Fahmi Rizki Syaban[3,4], Mirza Zaka Pratama[1,2*], Perdana Aditya Rahman[1,2] and Nabila Erina Erwan[3,4]

Abstract

Introduction The CXCR4 chemokine receptor is a G protein-coupled receptor that plays a role in many physiological processes and diseases, such as cancer metastasis, HIV infection, and immune response. Because of this, it may be possible to target it therapeutically. In addition, the active ingredient of *Phaseolus vulgaris* L (PVL) has been reported to have anti-inflammatory, antioxidant, and anticancer properties. Novel CXCR4 antagonists from natural resources can be a promising drug development product using a computational approach. This study aims to explore the active compound in PVL that has the responsibility to inhibit CXCR4 using molecular docking and dynamics simulation.

Materials and methods Pharmacokinetic analysis were performed using the pkCSM, OSIRIS for toxicity risk analysis, and the PerMM for membrane permeability assessment. Molecular docking was performed using PyRx software to determine the interaction between the CXCR4 target protein from the PDB database and the active component of PVL from the PubChem database. A molecular dynamics (MD) simulation was performed to determine the stability of the interaction using the WEBGRO Macromolecular Simulations online server. The analysis were performed by comparing the results with plerixafor as a control ligand.

Results and discussion The pharmacokinetic analysis of quercetin, kaempferol, myricetin, catechin, 3,4-dihydroxybenzoic acid, and daidzin in PVL showed that they met the drug-like criteria. These chemicals were expected to have medium-risk effects on mutagenesis and tumorigenesis, with the exception of catechin, which has no risk of toxicity, and daidzin, which has high-risk effects on mutagenesis and reproduction. Molecular docking identified that quercetin (−6.6 kcal/mol), myricetin (−6.6 kcal/mol), catechin (−6.5 kcal/mol), and 3,4-dihydroxybenzoic acid (−5.4 kcal/mol) bind to CXCR4 with the highest affinity compared to plerixafor (−5.0 kcal/mol) and can bind to the same binding pocket with key residues Asp187, Asp97, and Glu288. The MD simulation analysis showed that quercetin has a similar stability interaction compared to the control.

Conclusions Considering the pharmacokinetic analysis, molecular docking, and MD simulations, quercetin, myricetin, and 3,4-dihydroxybenzoic acid have the potential to become CXCR4 agonists with their good oral bioavailability and safety properties for the novel drug candidates. Future studies are needed to consider the molecular docking result.

*Correspondence:
Mirza Zaka Pratama
mirzazaka.pratama@gmail.com
Full list of author information is available at the end of the article

Introduction

The C-X-C motif chemokine receptor 4 (CXCR4) is a chemokine receptor that couples with G-proteins and is primarily expressed on endothelial cells and pericytes [1]. The activation is caused by the homeostatic chemokines stromal cell-derived factor-1 (SDF1, CXCL12), which initiates several biological processes [2, 3], including mesenchymal stem cell (MSC) mobilization to inflamed tissues [3, 4]. The interplay between CXCL12 and CXCR4 is complex and dependent on physiological and pathological conditions [2, 3]. Modulation of the CXCL12/CXCR4 axis contributes to disease progression, including cancer, autoimmune disease, and certain cardiac and neurological diseases [2].

CXCL12/CXCR4 is also involved in inflammation through several different pathways, such as PI3K/ AKT, NF-κB, and JAK/STAT [1, 3, 5, 6]. The CXCL12/CXCR4 pathway is crucial for the migration of various immune cells, including leukocyte trafficking, T and B cell migration and stimulation to their subtypes, inflammatory cytokine production [1], hematopoietic stem cell homing, survival, and maintenance in bone marrow [3]. The maintenance of activated immune cells by the CXCL12/CXCR4 pathway contributes to chronic inflammation in autoimmune inflammatory arthritis. The NF-kB activation and ERK phosphorylation pathways simulate IL-6, which subsequently promotes osteoclastogenesis [1]. Additionally, CXCL12 enhances apoptotic resistance and attracts the precursors of osteoclasts, contributing to an increase in bone-resorbing activity and cartilage destruction [7]. Based on the existing evidence regarding the role of CXCL12/CXCR4 in different diseases, there is a potential need to develop inhibition agents for this axis.

Several studies have revealed that the extracellular region of CXCR4 contains a significant negative potential, including crucial negatively charged residues (Asp187, Asp97, Asp262, and Glu288) that make up the essential binding region for its native ligand, CXCL12 [8, 9]. AMD3100 (Plerixafor), a synthetic antagonist for CXCR4, has significant potential and can strongly bind to specific residues for CXCR4 interaction. A recent NMR study showed that the CXCR4 antagonist AMD3100 could displace the CXCL12 N-terminus from the receptor without displacing the chemokine core domain [10, 11]. Previous studies also indicated that AMD3100 can mobilize stem cells to the peripheral blood [12]. Moreover, various studies have shown that the administration of AMD3100 can stimulate stem cell mobilization, inhibit CXCL12-induced angiogenesis, and reduce inflamed vessels in rheumatoid arthritis, all of which can contribute to the regeneration of damaged bone tissue [2, 12–14]. However, in addition to its high-cost [15], AMD3100 is not widely available in many developing countries, including Indonesia. Intravenous injection administration poses significant challenges and has numerous immediate side effects. Therefore, studying new antagonists for CXCR4 from herbal medicine is one of the strategies to reduce cost and can be widely distributed worldwide.

Phaseolus vulgaris L., also known as black beans, is a popular dietary source that is widely distributed in Indonesia and belongs to the legume family. *P. vulgaris* L. (PVL) beans are known for their high flavonoid content, which includes quercetin, kaempferol, myricetin, genistein, and tannic acid [16, 17]. Several studies have demonstrated that PVL exhibits anti-inflammatory, antioxidant, and anticancer properties, as well as lipid and glucose-lowering properties. PVL extracts in water and acetone can reduce inflammation by blocking TNF-α and CXCR4 [17, 18]. Moreover, PVL extract facilitates MSC homing and differentiation in the pancreatic tissue [19]. This study aims to explore the active constituent from PVL that is responsible for inhibiting CXCR4 using molecular docking and dynamics simulation.

Material and methods

Data mining of active compounds in *P. vulgaris* L.

We obtained the bioactive compounds of PVL from the literature review [20]. Additionally, PubChem ID, Molecular formula, and 2D structure were gathered for each compound.

ADMET, druglikeness, and membrane permeability

The active compounds in PVL underwent pharmacokinetic evaluation for compliance with Lipinski's Rule of Five (RoF) using the pkCSM website (https://biosig.lab.uq.edu.au/pkcsm/prediction). The data collected included molecule weight (MW), hydrogen bond acceptor (HBA), hydrogen bond donor (HBD), partition coefficient (LogP), and molecule refractivity [21]. Additionally, we assessed the toxicity of each compound using the OSIRIS application. The values of mutagenic, tumorigenic, irritant, and reproductive effects were collected from OSIRIS (16). The toxicity risk was then categorized with values of 0 (high risk), 0.5 (moderate risk), and 1 (safe) [22].

The membrane permeability was assessed using PerMM (https://permm.phar.umich.edu/permm_server_cgopm). The PerMM web server and database allow quantitative investigation and visualization of the passive translocation of bioactive chemicals across lipid membranes. A groundbreaking physics-based web tool, the server calculates membrane binding energies and permeability coefficients for a wide range of compounds on the phospholipid layer, PAMPA-DS, blood–brain barrier, and Caco-2/MDCK cell membranes. This study also visualizes transmembrane

translocation pathways, showing the successive translational and rotational positions of a permeant as it passes through the lipid layer. This study also illustrates the change in solvation energy resulting from this process. The server predicts permeability coefficients for compounds with many chemical scaffolds. Selection and optimization help identify and improve drug leads [23].

Protein–protein analysis of CXCR4 and CXCL12

We performed protein–protein interaction prediction between CXCR4 and CXCL12 because there is no experimental structure interaction between CXCR4 and CXCL12 in a database. Previous research by Xu et al. [10] predicted the interaction of CXCR4 and CXCL12 using ZDock. In this research, we generate an AI (artificial intelligence) prediction model using AlphaFold2 Multimer. We used CXCR4 and CXCL12 from the protein database (CXCR4: 3ODU; CXCL12: 4UAI), then input the amino acid sequences into AlphaFold2 Multimer and set them as default settings. The AlphaFold2 system will predict the structure and save it as a PDB file [24, 25].

Molecular docking analysis

Molecular docking was performed using PyRx 0.95 software on a computer with the Windows 10 operating system, 8 GB of RAM, a 500 GB NVME SSD, and an AMD Athlon 3150U CPU. The three-dimensional structures of every compound were obtained through the PubChem website (https://pubchem.ncbi.nlm.nih.gov/) and saved in a (.sdf) format file. The CCR4 as the protein target used in this study was obtained from the Protein Data Bank database (PDB) with protein ID 3ODU (https://www.rcsb.org/) [26, 27]. The three-dimensional structure of the protein was downloaded in PDB format. The downloaded proteins were stabilized by removing water, ligands, and hydrogen using PyMOL 2.0 software (https://pymol.org/2/) [28, 29]. The binding affinity interaction prediction was calculated using the Vina Wizard integrated with PyRx 9.5, using a specific grid box with the center coordinates and dimensions shown in Table 1. Since plerixafor is an inhibitor of CXCR4, we used plerixafor as a control in this study. The coordinates were chosen based on the location of a binding pocket and the residue interaction identified in the literature review [30, 31]. The protein–ligand interaction was visualized using UCSF ChimeraX (https://www.cgl.ucsf.edu/chimerax/) and Discovery Studio 2021 (https://discover.3ds.com/discovery-studio-visualizer-download) to discover the binding site and type of molecular interactions [32, 33].

Molecular dynamic (MD) *simulation*

Molecular dynamics simulations are an effective technique for understanding the structure–function relationships of macromolecules. In this research, molecular dynamics simulations were performed using the WEBGRO Macromolecular Simulations online server (https://simlab.uams.edu/ProteinWithLigand/index.html). This web is available free of charge to all researchers worldwide for academic purposes. Molecular dynamics simulations were performed for phytoconstituents that had a higher interaction affinity than the control. The first step for the MD simulations was to generate a topology of catechin, quercetin, kaempferol, myricetin, and hydroxybenzoic acid using the GlycoBioChemPRODRG2 server (http://davap.c1.bioch.dundee.ac.uk/cgi-bin/prodrg). The molecular dynamics simulation used GROMOS96 43a1 as the force field parameter, a temperature of 310 K, the addition of 0.15 M NaCl, 5000 steps of energy minimization, and a simulation time of 20 ns [34]. Parameters measured in this simulation include the root mean square distance (RMSD), the root mean square fluctuation (RMSF), and the number of hydrogen bonds.

Result

Phytochemical constituent of *P. vulgaris* L

The phytochemical constituent of PVL names, formulas, PubChem IDs, and SMILES representations are presented in Table 2. The compounds identified in this study include myricetin 3 glucoside, quercetin, quercetin 3 glucoside, kaempferol, myricetin, and kaempferol 3 glucoside, catechin, 3,4-dihydroxybenzoic acid, tannic acid, and daidzin.

Druglikeness and ADME prediction

The drug similarity of the PVL compounds was assessed using Lipinski parameters and other parameters listed in Fig. 1A. Pharmacokinetic properties were evaluated by ADME screening and are shown in Table 3.

Toxicity prediction

The toxicity prediction of the PVL compounds was assessed using OSIRIS software, as seen in Fig. 1B.

Table 1 Grid box docking dimension of study

Protein target	Center_X	Center_Y	Center_Z	Size_X (Ao)	Size_Y (Ao)	Size_Z (Ao)
CXCR4	20.609	−7.972	71.068	10	10	10

Table 2 List of PVL compounds

Comp. ID	Comp. class	Compounds name	PubChem ID	Molecular formula	Structure	References
F1	Flavonoid	Myricetin 3 Glucoside	44,259,426	$C_{21}H_{20}O_{13}$	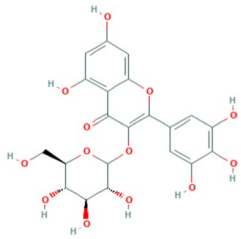	[17]
F2	Flavonoid	Quercetin	5,280,343	$C_{15}H_{10}O_7$	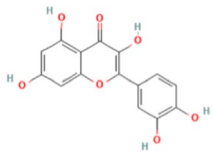	[17, 69]
F3	Flavonoid	Quercetin 3 glucoside	25,203,368	$C_{21}H_{19}O_{12}^{-}$	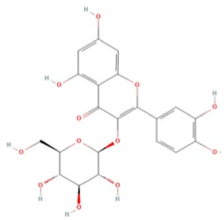	[17]
F4	Flavonoid	Kaempferol	5,280,863	$C_{15}H_{10}O_6$	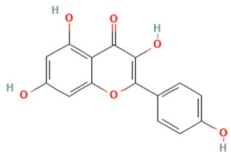	[69]
F5	Flavonoid	Myricetin	5,281,672	$C_{15}H_{10}O_8$	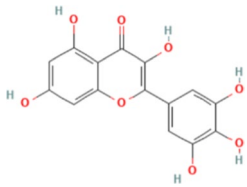	[69]
F6	Flavonoid	Kaempferol 3 glucoside	5,282,102	$C_{21}H_{20}O_{11}$	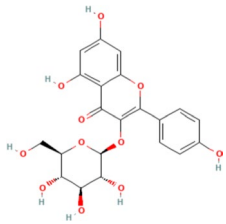	[17, 69]
F7	Flavonoid	Catechin	9064	$C_{15}H_{14}O_6$	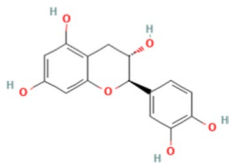	[69]
F8	Phenolic Acid	3,4-Dihydroxybenzoic acid	72	$C_7H_6O_4$	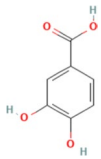	[69]

Table 2 (continued)

Comp. ID	Comp. class	Compounds name	PubChem ID	Molecular formula	Structure	References
F9	Flavonoid	Tannic Acid	16,129,778	$C_{76}H_{52}O_{46}$	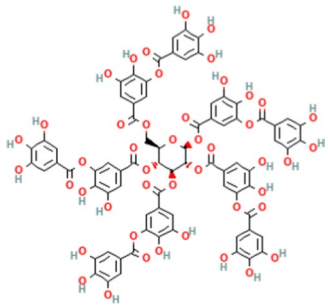	[35, 70]
F10	Flavonoid	Daidzin	107,971	$C_{21}H_{20}O_9$	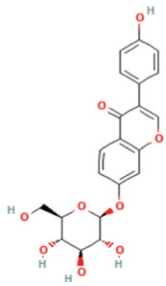	[69]
X	Synthetic CXCR4-antagonis	Plerixafor	65,015	$C_{28}H_{54}N_8$	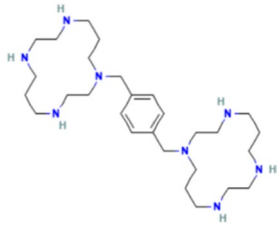	–

Membrane permeability prediction

The membrane permeability prediction of the PVL compounds was assessed using the PerMM web server, which can be seen in Fig. 1C for visualization and Fig. 1D for quantification.

Identification of CXCR4 and CXCL12 interaction and plerixafor inhibition site

To determine the binding mode interaction between CXCL12 and CXCR4, we generated an AlphaFold 2 multimer prediction structure as shown in Fig. 2a. Plerixafor binds to the same binding pocket with CLXCL12 as shown in Fig. 2B.

Molecular docking

To determine the interaction of active constituents of PVL against CXCR4, we generated molecular docking. We analyzed myricetin-3-glucoside, quercetin, quercetin-3-glucoside, kaempferol, myricetin, kaempferol-3-glucoside, catechin, 3,4-dihydroxybenzoic acid, daidzin, and tannic acid binding affinity interactions against CXCR4. The binding affinity interaction between the PVL chemical constituent and CXCR4 is shown in Fig. 3A.

The binding pocket interaction between the active constituents of PVL and CXCR4 was analyzed and compared with the amino acid residues formed with plerixafor. Quercetin, myricetin, kaempferol, catechin, and 3,4-dihydroxybenzoic acid can bind in the same binding pocket compared to the control in the presence of Asp187, Asp97, and Glu288 as critical amino acid residues, as shown in Fig. 3B. To know the specific interactions that occur in the interaction between the active constituent of PVL and CXCR4, we visualize the interaction using Discovery Studio. The interaction of the active constituent of PVL against CXCR4 is shown in Fig. 5A–E.

Molecular dynamics simulations

To determine the stability of the interaction, we performed a molecular dynamics simulation using the WEBGRO web server for as long as 20 ns. We visualization of post-MD interaction as shown in Fig. 5F–J. The root mean square distance (RMSD), the root mean square

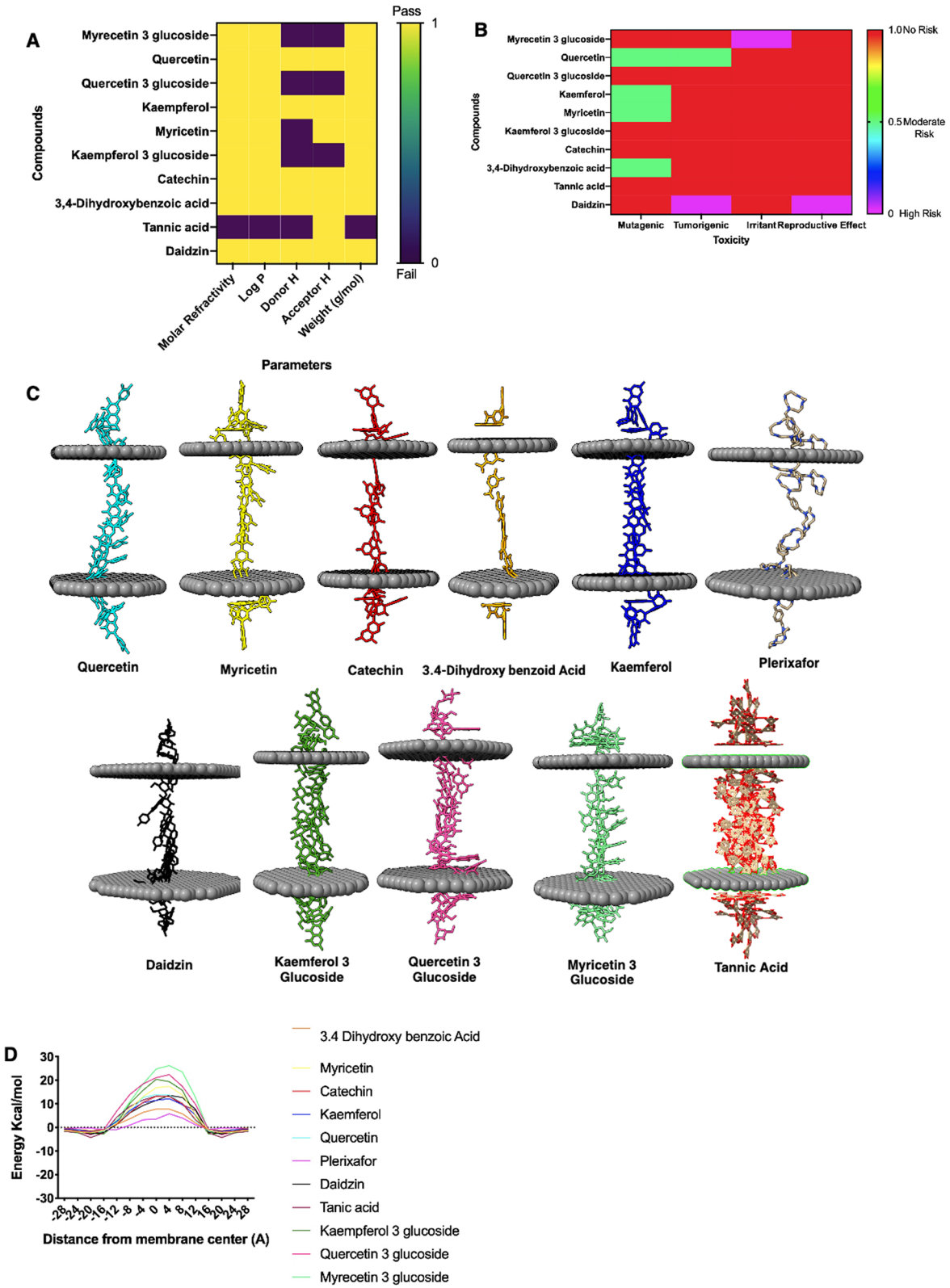

Fig. 1 **A** Lipinski RoF criteria analysis showed by yellow and black code indicating fulfilled or not fulfilled the criteria; > 1 parameters fail indicated not pass the criteria. **B** Toxicity analysis of the compounds against mutagenic, tumorigenic, irritant, and reproductive effects parameter categorized by 0 (high risk) (magenta), 0.5 (moderate risk) (light green), and 1 (safe) (red); **C** Anti-inflammatory probability activity analysis of all compounds; D) Permeability analysis showing the transfer energy for the compounds across the bilayer membrane

Table 3 Pharmacokinetic of PVL prediction

Pharmacokinetic property	Computationally predicted values for the phytochemicals (ADMET profile)													Measurement units
	Parameters	Reference Value	F1	F2	F3	F4	F5	F6	F7	F8	F9	F10	X	
Lipinski rule of 5	Molecular Weight	≤500	480.378	302.238	463.371	286.239	318.237	448.38	290.271	154.121	1701.206*	416.382	502.78	Numeric (g/mol)
	Acceptor Hydrogen	≤10	13*	7	12*	6	8	11*	6	3	46*	9	8	Numeric (AH)
	Donor Hydrogen	≤5	9*	5	7	4	6	7	5	3	25*	5	6	Numeric (DH)
	LogP	≤5	−0.8333	1.988	−1.1709	2.2824	318.237*	−0.2445	1.5461	0.796	4.8381	0.3443	0.68	Numeric (MLogP)
Absorption	Water solubility	< 0,4 mol/L (low) 0,4–41 mol/L (Medium) > 41 mol/L (high)	−2.904*	−2.925*	−2.848*	−3.04*	−2.915*	−2.863*	−3.117*	−2.069*	−2.892*	−2.784*	−2.841	Numeric (mol/L)
	Caco2 permeability	> 0.90	−1.34*	−0.229*	0.336*	0.032*	0.095*	0.306*	−0.283*	0.49*	−3.581*	0.24*	0.801	Numeric (Papp in 10^{-6} cm/s)
	Intestinal absorption (human)	Low: 0–20% Medium: 20–70% High: 70–100%	33.394	77.207	42.972	74.29	65.93	48.052	68.829	71.174	0*	59.319	50.545	Numeric (% Absorbed)
	Skin Permeability	Likely skin permeable: > -2.5	−2.735	−2.735	−2.735	−2.735	−2.735	−2.735	−2.735	−2.727	−2.735	−2.736	−2.735	Numeric (log K_p)
	P-glycoprotein substrate	Yes	Yes	Yes	Yes	Yes	Yes	Yes	Yes	No*	Yes	Yes	Yes	Categorical (Yes/No)
	P-glycoprotein I inhibitor	No	No	No	No	No	No	No	No	No	No	No	No	Categorical (Yes/No)
	P-glycoprotein II inhibitor	No	No	No	No	No	No	No	No	No	Yes*	No	No	Categorical (Yes/No)
Distribution	VDss (human)	Low: < -0.15 High > 2.81	1.542	1.559	1.423	1.274	1.317	1.444	1.027	−1.298*	0.011	−0.166*	1.2	Numeric (log L/kg)
	Fraction unbound (human)	–	0.265	0.206	0.215	0.178	0.238	0.218	0.235	0.648	0.381	0.199	0.571	Numeric (Fu)
	BBB permeability	Low: < 0.1 Medium: 0.1–0.2 High: > 0.2	−2.078*	−1.098*	−1.491*	−0.939*	−1.493*	−1.514*	−1.054*	−0.683*	−8.62*	−1.232*	−0.425	Numeric (log BB)
	CNS permeability	> -2 (penetrate BBB) < -3 (Can't penetrate BBB)	−4.747	−3.065	−4.068	−2.228	−3.709	−3.908	−3.298	−3.305	−8.582	−3.584	−2.871	Numeric (log PS)

Table 3 (continued)

Pharmacokinetic property	Computationally predicted values for the phytochemicals (ADMET profile)													Measurement units
	Parameters	Reference Value	F1	F2	F3	F4	F5	F6	F7	F8	F9	F10	X	
Metabolism	CYP2D6 substrate	No	No	No	No	No	No	No	No	No	No	No	No	Categorical (Yes/No)
	CYP3A4 substrate	No	No	No	No	No	No	No	No	No	No	No	Yes	Categorical (Yes/No)
	CYP1A2 inhibitor	No	No	Yes*	No	Yes*	Yes*	No	No	No	No	No	No	Categorical (Yes/No)
	CYP2C19 inhibitor	No	No	No	No	No	No	No	No	No	No	No	No	Categorical (Yes/No)
	CYP2C9 inhibitor	No	No	No	No	No	No	No	No	No	No	No	No	Categorical (Yes/No)
	CYP2D6 inhibitor	No	No	No	No	No	No	No	No	No	No	No	No	Categorical (Yes/No)
	CYP3A4 inhibitor	No	No	No	No	No	No	No	No	No	Yes*	No	No	Categorical (Yes/No)
Excretion	Total Clearance	−0.002	0.413*	0.407*	0.215*	0.477*	0.422*	0.462*	0.183*	0.551*	0.477*	0.104*	0.194	Numeric (ml/min/kg)
	Renal OCT2 substrate	No	No	No	No	No	No	No	No	No	Yes*	No	No	Categorical (Yes/No)
Toxicity	AMES toxicity	No	No	No	No	No	No	No	No	No	No	No	No	Categorical (Yes/No)
	hERG I inhibitor	No	No	No	No	No	No	No	No	No	No	No	No	Categorical (Yes/No)
	hERG II inhibitor	No	Yes*	No	Yes*	No	No	No	No	No	Yes*	Yes*	Yes	Categorical (Yes/No)
	Hepatotoxicity	No	No	No	No	No	No	No	No	No	No	No	No	Categorical (Yes/No)
	Skin Sensitization	No	No	No	No	No	No	No	No	No	No	No	No	Categorical (Yes/No)
	T. Pyriformis toxicity	Non-toxic: > 0.5 Toxic: < 0.5	0.285*	0.288*	0.285*	0.312*	0.286*	0.285*	0.347*	0.273*	0.285*	0.285*	0.241	Numeric (log µg/L)

* : Aestheric indicated not match as the reference value

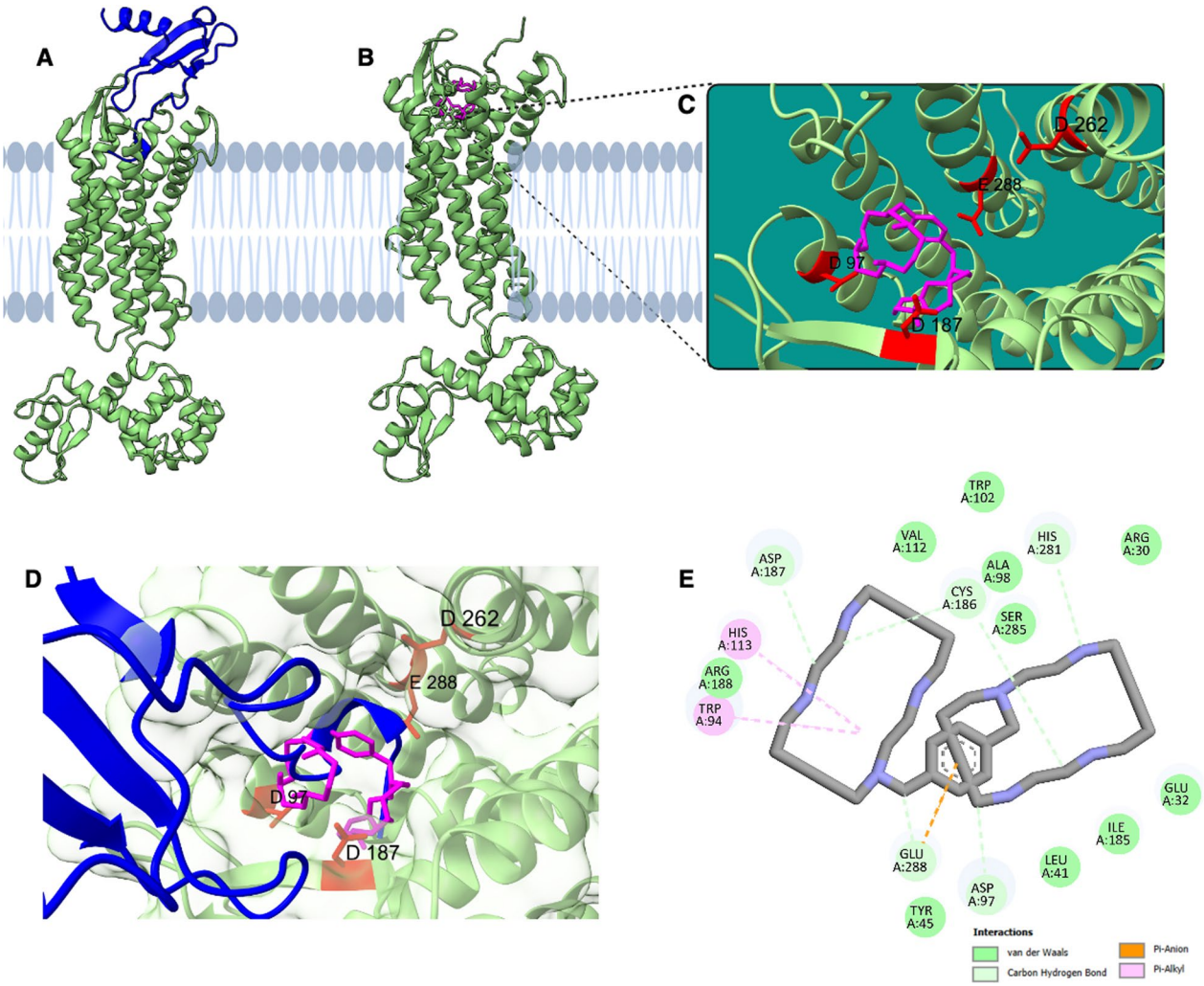

Fig. 2 **A** Interaction of CXCR4 (green) and CXCR12 (blue) as a native ligand; **B** Interaction of CXCR4 (green) and Plerixafor (magenta) as a control ligand; **C** CXCR4-Plerixafor interaction through three critical residues (red))(Asp97, Asp187, Asp262, and Glu288); **D** Superimposed interactions between CXCR4, CXCL12, and Plerixafor; **E** 2D visualization interaction of plerixafor against CXCR4 using Discovery studio

fluctuation (RMSF), and the number of hydrogen bond results can be seen in Fig. 6.

Discussion

Phytochemical constituent of *P. vulgaris* L

The phytochemical constituents of PVL have been explored in some varieties of PVL influenced by distributed area of origin, environmental conditions, or method of extractions [17, 20, 35]. Different studies reported the phytochemical content of PVL, such as saponin, anthocyanins, flavonols, phenolic acids, proanthocyanidins, and other bioactive compounds, as well as its evidence for anti-inflammatory, anticancer, and immunomodulatory agent [17, 20, 36, 37] as summarized in Table 2. The compound with the highest binding affinity will be selected for molecular dynamic simulations analysis as shown in Fig. 5.

Druglikeness, and ADME prediction toxicity prediction of phytochemical constituents of *P. vulgaris* L

To know the prediction of pharmacokinetics for each chemical component of PVL, we analyzed the Rule of Five (RoF) score. PVL active compounds were retrieved in sdf file format from the PubChem database (http://pubchem.ncbi.nlm.nih.gov/). Our study revealed that quercetin, kaempferol, myricetin, catechin, 3,4-dihydroxybenzoic acid, and daidzin contained in PVL met the RoF criteria. Besides, other compounds did not meet the RoF criteria due to some factors such as MW > 500, HBA > 10, and LogP > 5, as shown in Fig. 1A and Table 3.

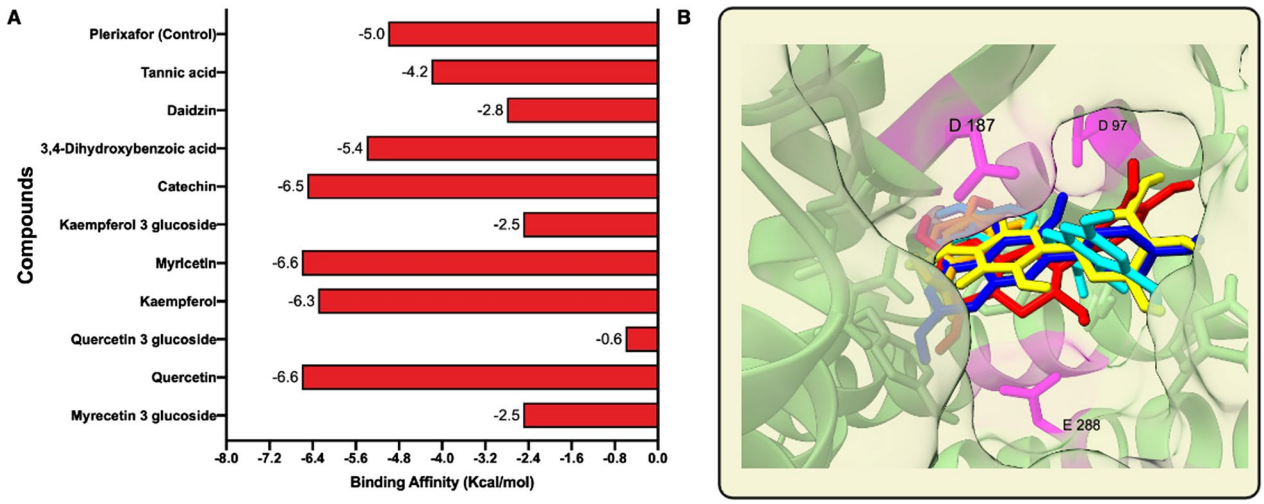

Fig. 3 **A** Binding affinity from molecular docking result of CXCR4 and the ligand compounds compared to ligand control; **B** Catechin (Red), Kaempferol (blue), Myricetin (yellow), Quercetin (cyan) and 3,4-Dihydroxybenzoic acid (orange) interact with CXCR4 in the same binding pocket

RoF is a criterion for evaluating the similarity of a compound to a drug. The requirements for RoF are that the hydrogen bond acceptor (HBA) must be less than 10, the hydrogen bond donor (HBD) must be less than 5, the molecular weight (MW) must be less than 500 g/mol, the H2O partition coefficient (LogP) must be less than 5, and the molar refractivity must be between 40 and 130. The compounds that meet the RoF are predicted to have drug-like properties [38].

Pharmacokinetic properties, including absorption, distribution, metabolism, and excretion, were analyzed among the active compounds of PVL, as shown in Table 3. In absorption, solubility and permeability are essential drug-specific physicochemical properties related to the ability of the drug across the membrane to reach the desired concentration in the systemic circulation [39]. Solubility is critical in developing oral drugs, as low solubility can affect intestinal absorption through the portal circulation. Notably, all PVL compounds have low water solubility (< 0.4 mol/L), indicating poor water solubility related to lipophilicity since they have LogP less than 5 [40]. Low water solubility can lead to a poor dissolution rate and potentially limit intestinal absorption, whereas high lipophilicity can enhance the intestinal absorption of a drug. Other factors like permeability and formulation play significant roles in determining the overall bioavailability of a drug. Strategies such as the use of surfactants, lipids, permeation enhancers, micronization, salt formation, nanoparticles-drug delivery system, and solid dispersions are employed to overcome issues related to poor aqueous solubility and enhance the bioavailability of lipophilic drugs [41–43]. Thus, PVL compounds can be potentially used as oral administration drugs. However, further studies are needed to optimize the absorption capacity for future drug development.

It is noteworthy that all PVL compounds have low water solubility (< 0.4 mol/L), indicating poor water solubility related to lipophilicity. However, all compounds have high intestinal absorption in humans, indicating the percentage of drug absorption in the small intestine. Thus, further studies to optimize the absorption capacity are needed for future drug development.

The distribution property shows the distribution of drugs within different body compartments. All PVL drugs have a low blood–brain barrier (BBB) (< 0.1 log BB) and central nervous system (CNS) permeability (< −3 log PS), indicating that they cannot penetrate the BBB. Metabolic property is another essential factor that affects a drug's pharmacokinetics, pharmacodynamics, and safety profile. Cytochrome P450 is a primary component in drug metabolism located in the liver and intestine and is either induced or inhibited by various substances [40]. Most of the compounds contained in PVL do not inhibit the cytochromes, except for CYP1A2 and CYP3A4 in several substances as shown in Table 3.

Toxicity prediction of phytochemical constituents of *P. vulgaris* L

Toxicity analysis is an essential parameter in determining the safety of compounds. To know the safety of each compound, we predicted the possibility of toxicity using the OSIRIS software, which used some parameters such as mutagenic, tumorigenic, irritant, and reproductive effects. Mutagenic and tumorigenic are parameters to predict the effect of the compound on becoming mutagenic and causing tumors. As a result, most PVL

compounds are safe for toxicity analysis instead of quercetin, kaempferol, myricetin, 3,4-dihydroxybenzoic acid, and daidzin. These compounds were predicted to have medium-risk mutagenic and tumorigenic effects, except for daidzin, which has high-risk tumorigenic and reproductive effects. In addition, myricetin-3-glycoside, quercetin-3-glycoside, kaempferol-3-glycoside, catechin, and tannic acid have no risk for toxicity analysis, as shown in Fig. 1B. Nevertheless, wet lab studies are required to determine the optimal dosage, and a significant risk depends on the amount (16).

Membrane permeability prediction phytochemical constituents of *P. vulgaris* L

The ability of compounds to penetrate the membrane revealed that the compound with the lowest transfer energy along the translocation pathways identified by its calculated transfer energy profile is more permeable across the bilayer membrane [23]. To know the membrane penetration ability of each compound, we predicted using the PerMM web server. Figure 1C is a visualization of the conformational change of the PVL active compounds as they penetrated the cell membrane. Each molecule continuously adjusted its position to match the hydrophilic and hydrophobic characteristics of the plasma membrane. The analysis showed that plerixafor had the lowest energy across the membrane. Among the compounds contained in PVL, 3,4-dihydroxybenzoic acid has the lowest energy to cross the membrane, followed by kaempferol, daidzin, catechin, tannic acid, quercetin, myricetin, kaempferol-3-glucoside, quercetin-3-glucoside, and myricetin-3-glucoside, as shown in Fig. 1D.

Hydrophobic (non-polar) compounds can easily penetrate the lipid bilayer. Hydrophilic (polar) molecules, on the other hand, typically rely on transport proteins to cross the membrane because they cannot easily penetrate the hydrophobic interior of the bilayer [23]. Typically, the ligand for CXCR4 does not enter the membrane. Instead, it attaches to the extracellular region of the receptor, inducing a structural change that transmits a signal throughout the cell.

CXCR4 and CXCL12 binding mode interaction and plerixafor as inhibitor

The protein–protein interaction results were then analyzed for quality using Ramachandran plots via the PROCHECK web server. A good quality model was confirmed based on residues in the most favored regions (> 90%), as shown in Additional file 1: Fig. S1. The interaction appears to be similar to previous studies in that CXCL12 bound to the extracellular region of CXCR4 contains a significant negative potential, including critical negatively charged residues at residues Asp187, Asp97, Asp262, and Glu288 [10, 11].

As we mentioned in the introduction plerixafor is a CXCR4 inhibitor. The visualization interaction between plerixafor and CXCR4 shows that it can bind to the extracellular region of CXCR4 (Fig. 2B) at Asp187, Asp97, and Glu288 residue, but slightly far from Asp262 residue as shown in Figs. 2C. The mechanism by which SDF-1 binds to CXCR4 involves the interaction of the N-terminus domain of SDF-1 with the extracellular domain CXCR4, followed by further interactions that stabilize the complex and lead to signal transduction. Superimposed interaction shows that plerixafor has a binding mode similar to CXLC12. This binding mode curled up in the CXCR4 extracellular binding pocket of the CXCr4 [44] as shown in Fig. 2D. 2D interaction shows that plerixafor can bin to CXCR4 by forming hydrogen bond at Glu288, Tyr45, Asp97, Leu41, Ile185, Arg30, His281, Ala98, Ser285, Cys186, Trp102, Val112, Asp187, Arg188; hydrophobic bond at His113 and Trp94 as shown in Fig. 2E. As we mention before that Glu288, Asp187 and Asp97 is important residue in binding interaction CXCR4/CXCL12, indicating the reasonable of plerixafor as an established drug for CXCR4 antagonist. Moreover, Plerixafor is the only CXCR4 antagonist approved by the FDA and has been commercially distributed. Several studies have developed potential candidates for synthetic CXCR4 antagonists, such as POL6326 (Balixafortide), LY2510924, TN14003, and MSX-122, which exhibit good safety and tolerability profiles yet are still in preclinical and clinical studies phases [45–47]. So, we used plerixafor as the control ligand in this study.

Molecular docking before and after dynamics simulation of *P. vulgaris* L active constituent against CXCR4

A molecular docking study is a research model used in drug discovery to determine the binding interaction between ligand and protein [48]. The binding affinity measures the strength of the interaction between two molecules [49]. Our molecular docking analysis identified that quercetin (−6.6 kcal/mol), myricetin (−6.6 kcal/mol), kaempferol (−6.3 kcal/mol), catechin (-6.5 kcal/mol), and 3,4-dihydroxybenzoic acid (−5.4 kcal/mol) bind to CXCR4 with the highest affinity compared to plerixafor (−5.0 kcal/mol) as the control ligand. The remaining compounds with the lowest affinity compared to the control ligand are myricetin-3-glucoside (−2.5 kcal/mol), quercetin-3-glucoside (−0.6 kcal/mol), kaempferol-3-glucoside (−2.5 kcal/mol), daidzin (−2.8 kcal/mol), and tannic acid (−4.2 kcal/mol), with lower affinity compared to plerixafor. The molecule with the lowest binding energy will have a constant temperature and pressure, called a stable molecule. The amino

acid residues influenced the binding domain of the target protein and the type of chemical interactions in the binding region [50]. A lower energy value of binding affinity denotes a more stable and favorable binding relationship between the target protein and the ligand [49]. However, further experimental studies are necessary to confirm the actual protein–ligand interaction [51].

The interaction between catechin and CXCR4 formed a hydrogen bond at Glu32, Leu41, Tyr45, Val112, Tyr116, Arg183, Ile185, Ser285, and Glu288; a hydrophobic bond at Trp94, Ala98, and Asp97 and His113 (Fig. 5A). In addition, myricetin binds to CXCR4, forming a hydrogen bond with Arg30, Glu32, Phe93, Trp94, Asp97, Trp102, Val112, Tyr126, Ser285, and Arg188; a hydrophobic bond with His113, and an unfavorable donor bond with His281 (Fig. 5B), while, 3,4-dihydroxybenzoic acid can interact through binding interactions with Trp102, Val112, Tyr116, Asp97, Arg188, Hlu288 via hydrogen, Trp94 via hydrophobic, and His113 via pi-anion bonds (Fig. 5C). Kaempferol interactions at Arg30, Glu32, Asp97, Val112, Arg188, His281, and Ser285 as hydrogen bonds; Trp94 and Tyr116 as hydrophobic bonds; and His113 and Glu288 as pi-anion bonds (Fig. 5D). Kaempferol and plerixafor have the same binding interaction in Trp94 via a hydrophobic bond and in Glu288 via a pi-anion bond. Then, the quercetin-CXCR4 interaction formed a hydrogen bond at Leu42, Tyr45, Val112, Tyr116, His281, Asp187, Ser285, and Glu288; a hydrophobic bond at Trp94 and His113; and a pi-anion bond with Asp97 (Fig. 5E). All compounds have similar interactions compared to plerixafor. They can bind at least in Asp97 and Glu288, which have critical binding in the CXCL12/CXCR4 interaction.

Molecular dynamic simulations were performed for 20 ns to evaluate the structural behavior of the lead compounds within the substrate-binding active cavity of CXCR4. Plerixafor post-MD interaction forms a hydrogen bond at Arg30, Thr90, Phe93, Asp97, Trp102, Cys109, Val112, Arg188, Tyr190, Ile284, Gln200, Asp262, and Glu288; hydrophobic bond at Trp94, His113, Tyr116 and Cys186 as shown in Fig. 4. Cathecin post-MD interaction forms a hydrogen bond at Phe87, Leu91, Thr90, Phe93, Cys109, Cys186, His113, Ile185, Tyr255, Ile259, and Phe292; a hydrophobic bond at Trp94, Trp102, Tyr116, and Val112 (Fig. 5F). While myricetin, post-MD simulation, forms a hydrogen bond with Thr90, Phe93, Asp97, His113, Ala175, Asn176, Cys186, Asp187, Arg188, Glu288; and a hydrophobic bond with Trp94, Trp102, Val112, and Tyr116 as shown in Fig. 5G. 3,4-dihydroxybenzoic acid post-MD interaction is formed via a hydrogen bond with Thr90, Phe93, Asp97, Trp102, His113, Tyr116, Cys186; and a hydrophobic bond with Trp94 and Val112 (Fig. 5H). In addition, based on MD simulations, kaempferol-CXCR4 interacts by forming a hydrogen bond with Phe13, Glu15, Ser16, Trp57, Leu55, and Val18; and a hydrophobic bond with Phe14 (Fig. 5I), while quercetin post-MD simulation formed a hydrogen bond at Ser28, Leu41, Tyr45, Val112, Tyr116, and Arg188; a hydrophobic bond at Trp94 and Ala98; and a pi-anion bond with Asp97 and His113 (Fig. 5J). Post-MD interaction analysis showed that quercetin, myricetin, and 3,4-dihydroxybenzoic acid still can bind to critical amino acid residue at Asp97, Asp187, and Glu288 as shown in Table 4 and Fig. 5. The stability of the CXCR4 protein refers to the collective pressures determining whether the protein will maintain its folded shape or adopt non-native aggregating configurations. Comparing the structure of protein–ligand complexes at different levels of stimulation up to 20 ns provides valuable structural insights that help to understand the potential changes in ligand position that occur as a result.

The protein–ligand interactions play a vital role in structural biology by providing insight into the mechanisms of these interactions at the molecular level. The similarity of the binding to the control indicates the same function. A similar interaction active constituent of PVL can be seen in Table 4. Identification of molecular interactions and binding orientations on the docked protein–ligand complex revealed that PVL compounds form non-covalent interactions with all target proteins through hydrophobic, pi, and hydrogen bonds. These interactions lead to the development of the protein–ligand complex and trigger the initiation of an activity response, including enhancement and inhibition of the target protein [22, 48]. Together with another additional factor, such as binding affinity (binding affinity analysis), the similarity of those interaction types between a natural compound and the control ligand (interaction analysis) could indicate the accuracy of the docking method and support the potential of a ligand as a drug candidate [52, 53]. The critical molecular interaction, hydrophobic, pi, and hydrogen bonds can help to stabilize the ligand within the protein's active site, leading to a stronger binding affinity and potentially inhibitory activity [53, 54]. The similarity interaction between the PVL compound and the control ligand (Plerixafor) suggests the potential inhibitory activity as a CXCR4 antagonist candidate. Since molecular docking solely is insufficient to conclude the promising activity, further methods such as molecular dynamic simulation will provide information about the stability and dynamics of the protein–ligand complex by optimizing the structures of the final complexes from docking, calculating detailed interaction energies, and providing information about the ligand binding mechanism [55], as we conducted in this study.

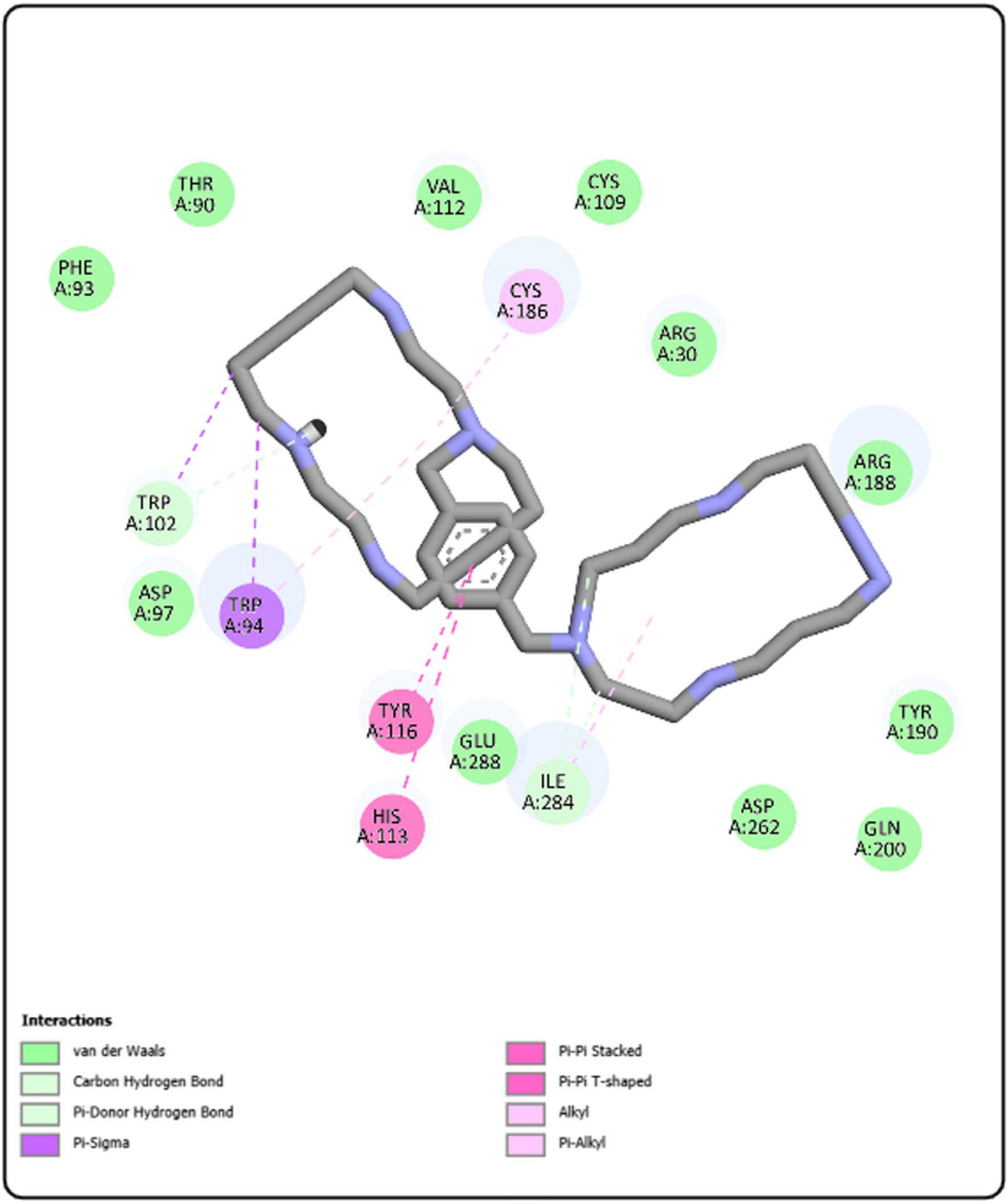

Fig. 4 2D Visualization post-MD (Molecular dynamic simulations) of Plerixafor against CXCR4

The molecular dynamics simulation

2D plots were generated to illustrate the varying behavior of the docked complex at different time intervals during the MD simulation runs. The plots play a critical role in the statistical analysis of the MD simulations. They provide valuable insight into the stability and flexibility of the residues at different time points during the simulations [56]. The RMSD results show a stable interaction between plerixafor and CXCR4. The value was approximately 0.3 nm from 0 to 20 ns. The active constituent of PVL, catechin RMSD, shows stability from 2 to 11 ns with an average RMSD value of 1.1 nm, then unstable fluctuation up to 20 ns. Myricetin shows instability from 0 to 20 ns with an average RMSD value of 1 nm,

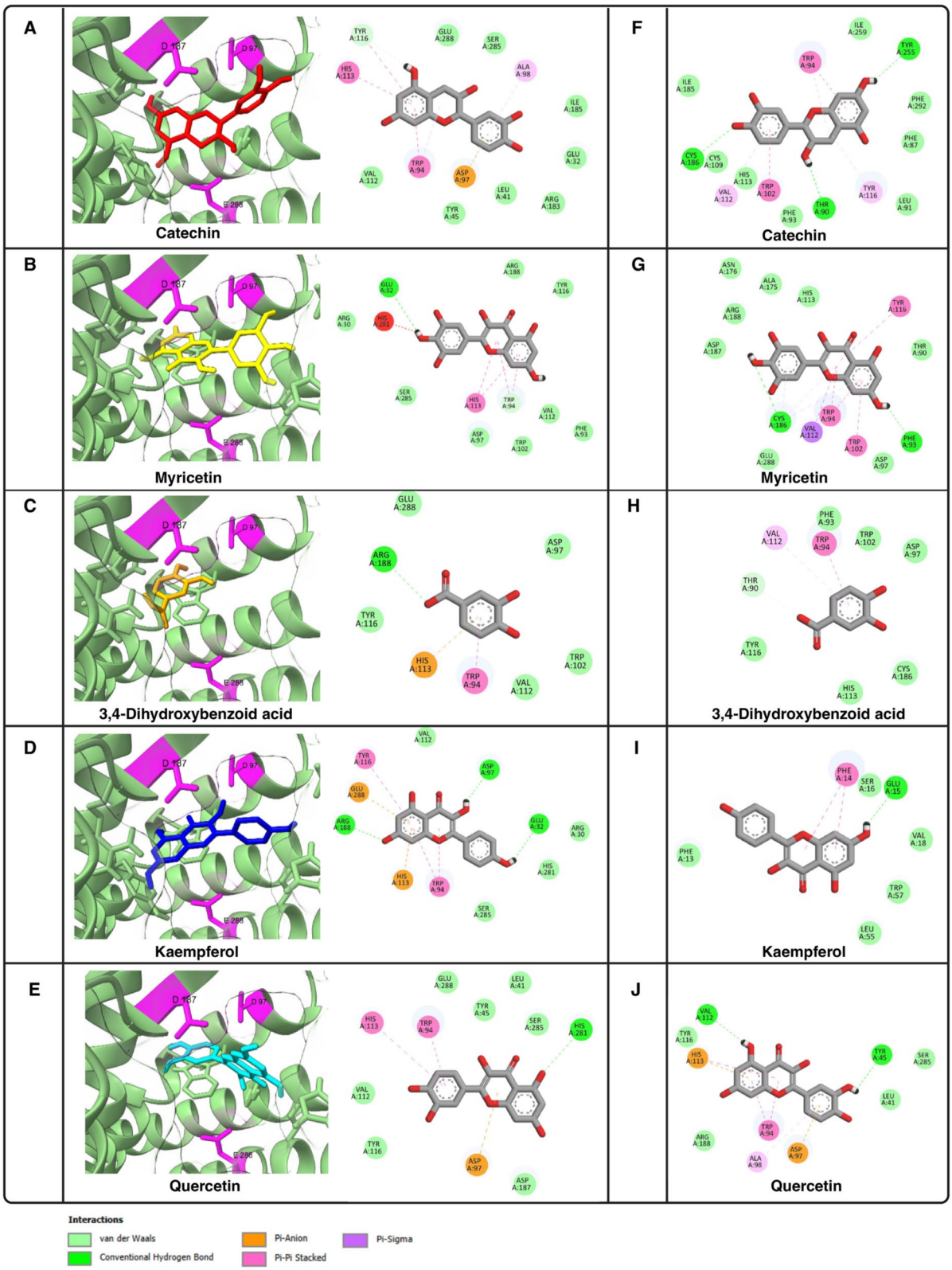

Fig. 5 Amino acid residues result from the interaction between ligands and CXCR4. Panels A to E show interaction before molecular dynamics, while panels F to J show residues after molecular dynamics simulations

Table 4 Molecular interaction active compound of *P. vulgaris L.* with CXCR4

Compounds	Molecular Interaction	Molecular interaction after MD
Quercetin	Hydrogen: **His281, Glu288, Asp187,** Val112, Tyr116, Tyr45, Leu41, Ser285	Hydrogen: Tyr45, Val112, Tyr116, Ser285, Leu41, Arg188
	Hydrophobic: Trp94, **His113**	Hydrophobic: Trp94, Ala98
	Pi-anion: **Asp97**	Pi-anion: **Asp97**, **His113**
Kaempferol	Hydrogen: Glu32, **Asp97**, Arg188, Ser285, His281, Arg30, Val112	Hydrogen: Glu15, Ser16, Val18, Trp57, Leu55, Phe13
	Hydrophobic: Trp94, Tyr116	Hydrophobic: Phe14
	Pi-anion: **His113**, **Glu288**	Pi-anion: -
Myricetin	Hydrogen: Glu32, Trp94, Arg188, Tyr116, Phe93, Val112, Trp102, **Asp97**, Ser185, Arg30	Hydrogen: Phe93, Cys186, **Asp97**, **Glu288**, Asp187, Arg188, Asn176, Ala175, **His113**, Thr90
	Hydrophobic: **His113**	
	Unfavorable: **His281**	Hydrophobic: Trp94, Trp102, Tyr116
		Pi-anion: Val112
Catechin	Hydrogen: Tyr116, **Glu288**, Ser285, Ile185, Glu32, Arg183, Leu41, Tyr45, Val112	Hydrogen: Cys186, Thr90, Tyr255, Cys109, **His113**, Phe93, Leu91, Phe87, Phe292, Tyr255, Ile259, Ile185
	Hyrophobic: Trp94, Ala98, **His113**	
	Pi-anion: **Asp97**	Hydrophobic: Trp102, Trp94, Tyr116, Val112
		Pi-anion: -
3,4 Dihydroxybenzoic acid	Hydrogen: Arg188, Tyr116, Val112, Trp102, **Asp97**, **Glu288**	Hydrogen: Thr90, Tyr116, **His113**, Cys186, **Asp97**, Trp102, Phe93
	Hydrophobic:Trp94	Hydrophobic: Trp94, Val112
	Pi-anion: **His113**	Pi-anion: -
Plerixafor (Control)	Hydrogen: Asp97, Cys186, Asp187, His281, Glu288	Hydrogen: Arg30, Thr90, Phe93, Asp97, Trp102, Cys109, Val112, Arg188, Tyr190, Ile284, Gln200, Asp262, and Glu288
	Hydrophobic: Trp113, His113	
	Pi-anion: Glu288	Hydrophobic: Trp94, His113, Tyr116 and Cys186

Bold: indicating similar binding with plerixafor as control

indicating that the interaction of myricetin with CXCR4 is unstable. 3,4-dihydroxybenzoic acid fluctuates from 0 to 6 ns and is stable from 6 to 20 with an RMSD score of 0.7 nm. Kaemferol was stable from 3 to 12 ns with an RMSD score of 0.4 nm, then fluctuated to 16 ns and stabilized at 20 ns. Interestingly, quercetin has a similar stability interaction with an average RMSD score of 0.3 nm from 0 to 20 ns, indicating that quercetin has a similar stability interaction compared to plerixafor, as shown in Fig. 6A.

The PVL compound causes significant fluctuations in amino acid residues in certain regions of the protein, as shown by the RMSF curve in Fig. 6B. Analysis of residue-specific root mean square fluctuation (RMSF) provides insight into how ligand binding affects the structural flexibility of a protein at the single amino acid level [57]. A higher RMSF value indicates greater flexibility of the complex. Leu68, Asp97, Leu146, and Thr178 have the largest backbone variation of 5 nm. The significant variations in amino acid residues suggest the fluctuating interactions between the compound and these residues, possibly involving hydrogen bonding, ionic interactions, or van der Waals forces. The PVL compounds appear to have a remarkable effect on the structure and dynamics of the protein, potentially serving as a modulator or regulator of important protein functions.

To explain the conformational stability of the interaction, we examine the total number of intermolecular hydrogen bonds in the ligand–protein complexes. Hydrogen bonds play an important role in the stability of the protein structure [55]. Interestingly, the number of hydrogen bonds in catechin, hydroxybenzoic acid, myricetin, and quercetin compounds has the same value as plerixafor, with an average of 380. but the number of hydrogen bonds in kaempferol compounds has a lower average of 320, as shown in Fig. 6C.

Future potential active constituent of PVL as CXCR4 inhibitor

PVL is rich in a variety of phytochemicals, including flavonoids, phenolic acids, and other antioxidants [17]. Some of these compounds have shown biological activity in various contexts, although their specific interaction with CXCR4 would require targeted research.

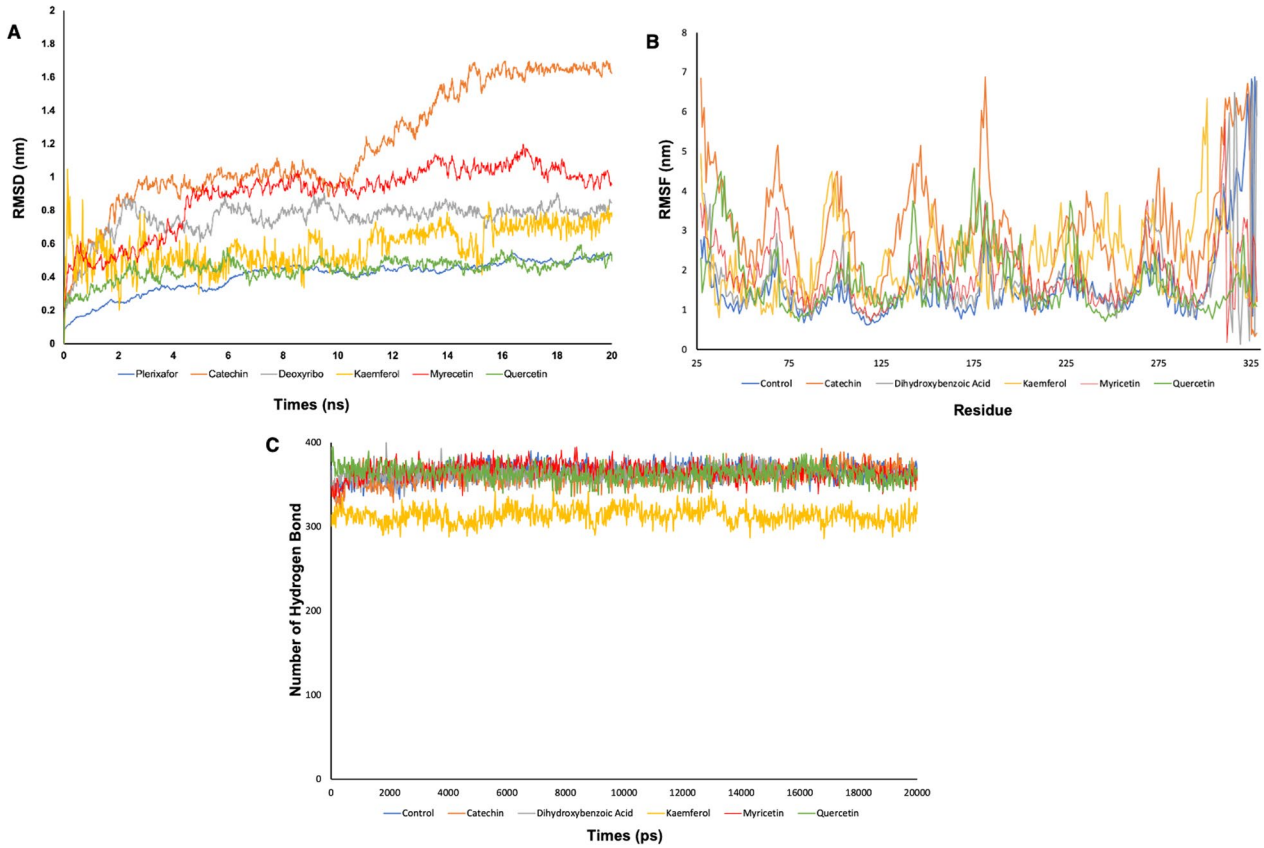

Fig. 6 The molecular dynamic of PVL against CXCR4. **A** Root Mean Square (RMSD), **B** Root Mean Square Fluctuation (RMSF), **C** Number of Hydrogen bond

The CXCR4/CXCL12 pathway has been proposed as a target for stem cell mobilization-based therapy in various rheumatic diseases. Several studies have reported that upregulation of CXCR4 and CXCL12 is associated with joint erosion, synovial inflammation, synovial hyperplasia, and synovial angiogenesis [58]. Mesenchymal stem cells have been shown to stimulate chondrocyte regeneration and differentiation into cartilage [59]. Osteoarthritis, stem cell-based treatment has shown promising clinical effects, including improved joint function, pain threshold, and quality of life [60]. In comparison, stem cell-based treatment can modify and restore the balance of inflammatory T cells in rheumatoid arthritis [61].

CXCL12/CXCR4 axis also has a potential therapeutic target for several inflammatory diseases, not only by affecting cell migration but also by altering the immune response. Only one antagonist targeting the CXCR4 ligand binding region, plerixafor, has shown therapeutic relevance (1). In addition, the role of chemokines in immune modulation in autoimmune diseases remains to be explored. Chronic diseases, especially autoimmune diseases such as rheumatoid arthritis (RA), inflammatory bowel disease (IBD), and systemic lupus erythematosus (SLE), are associated with an abnormal inflammatory response because the immune system recognizes the protein as an antigen and attacks itself [62–64].

This study shows that several candidate active constituents of PVL can potentially become CXCR4 inhibitors. Computational tools and molecular modeling can predict the interaction between potential phytochemicals in PVL against the CXCR4 receptor. Such in silico studies can be a cost-effective first step before experimental studies, but this finding needs to be clarified with more precise and advanced studies [65]. Any potential CXCR4 inhibitors identified would need to undergo rigorous preclinical and clinical testing to establish their safety and efficacy.

The efficacy of natural product derived-CXCR4 inhibitor flavonoids, isoflavones, bioketones, and isoprenoidyl has been observed through CXCR12/CXCR4 axis. Promising inhibitory activity of flavonoid compounds such as Quercetin [66, 67] and myricetin has been reported in downregulating CXCL12 and CXCR4 expression in prostate cancer [68]. However, further safety assessment is necessary to validate those efficacious activities of the novel CXCR4 antagonist. Research in CXCR4 antagonist development from

natural products is escalating despite the compound's pharmacokinetic, pharmacodynamic, and toxicity testing not being comprehensively studied, which is insufficient to replace the established agent Plerixafor.

We understand that there are limitations to this study. In our study, we only predicted the potential of the active component of PVL against CXCR4 using computational study. Therefore, we cannot confirm the effect of PVL on CXCR4 in experimental studies using cells or animals. At least, this research can support and serve as a basis for further research in vitro and in vivo. Further research is needed to clarify our predictive findings through experimental studies, such as examination of binding interaction and visualization using X-rays or cryo-EM. Experimental toxicity studies are also needed to confirm PVL as a candidate for CXCR4 inhibitor. It is important to note that while natural products are a promising source for drug discovery, the path from identifying a potential lead compound to developing a clinically approved drug is long, complex, and challenging. Any findings would need to be substantiated through rigorous scientific research and clinical trials. At this time, any potential CXCR4 inhibitory compounds in PVL remain speculative and would require significant research to validate.

Conclusion

In sum, virtual screenings of active constituents of PVL using molecular docking and dynamic simulation revealed that quercetin, myricetin, and 3,4-dihydroxybenzoic acid have the potential to become CXCR4 agonists. These three active constituents have good oral bioavailability and toxicity. Further research is required to fully understand and clarify PVL as a CXCR4 inhibitor.

Supplementary Information

The online version contains supplementary material available at https://doi.org/10.1186/s43042-024-00510-9.

Additional file 1. The result of protein-protein interaction by Ramachandran plot.

Acknowledgements
Not Applicabele.

Author contributions
CSW was involved in the conception and design of the audit, in data collection and analysis, and in the writing, revising, and reviewing of the manuscript. MFRS, MZP, PAR, and NEE were involved in the conception and design of the audit, and in the revising and reviewing of the manuscript. CSW, MFRS, and MZP confirm the raw data's authenticity. All authors have read and approved the final manuscript.

Funding
No funding was received.

Availability of data and materials
The datasets used for analysis during these studies were included in this published study.

Declarations

Ethics approval and consent to participate
Not applicable.

Patient consent for publication
Not applicable.

Competing interests
The authors declare that they have no competing interests.

Author details
[1]Rheumatology Division, Department of Internal Medicine, Faculty of Medicine, Universitas Brawijaya – Saiful Anwar General Hospital, Malang, Indonesia. [2]Dr. Saiful Anwar General Hospital, Jl. Jaksa Agung Suprapto No: 2, Malang 65111, Indonesia. [3]Faculty of Medicine, Brawijaya University, Malang, Indonesia. [4]Faculty of Medicine, Brawijaya University, Jl. Veteran, Malang 65145, Indonesia.

Received: 9 January 2024 Accepted: 14 March 2024
Published online: 10 April 2024

References

1. Mousavi A (2020) CXCL12/CXCR4 signal transduction in diseases and its molecular approaches in targeted-therapy. Immunol Lett 217:91–115
2. Huynh C, Dingemanse J (2020) Meyer zu Schwabedissen HE and Sidharta PN: relevance of the CXCR4/CXCR7-CXCL12 axis and its effect in pathophysiological conditions. Pharmacol Res 161:105092
3. García-Cuesta EM, Santiago CA, Vallejo-Díaz J, Juarranz Y, Rodríguez-Frade JM, Mellado M (2019) The role of the CXCL12/CXCR4/ACKR3 axis in autoimmune diseases. Front Endocrinol 10:1–16
4. Staudt ND, Maurer A, Spring B, Kalbacher H, Aicher WK, Klein G (2012) Processing of CXCL12 by different osteoblast-secreted cathepsins. Stem Cells Dev 21:1924–1935
5. Guo F, Wang Y, Liu J, Mok SC, Xue F, Zhang W (2016) CXCL12/CXCR4: a symbiotic bridge linking cancer cells and their stromal neighbors in oncogenic communication networks. Oncogene 35:816–826
6. Suzuki M, Mohamed S, Nakajima T et al (2008) Aberrant methylation of CXCL12 in non-small cell lung cancer is associated with an unfavorable prognosis. Int J Oncol 33:113–119
7. Zhou W, Guo S, Liu M, Burow ME, Wang G (2017) Targeting CXCL12/CXCR4 axis in tumor immunotherapy. Curr Med Chem 26:3026–3041
8. Brelot A, Heveker N, Adema K, Hosie MJ, Willett B, Alizon M (1999) Effect of mutations in the second extracellular loop of CXCR4 on its utilization by human and feline immunodeficiency viruses. J Virol 73:2576–2586
9. Brelot A, Heveker N, Montes M, Alizon M (2000) Identification of residues of CXCR4 critical for human immunodeficiency virus coreceptor and chemokine receptor activities. J Biol Chem 275:23736–23744
10. Xu L, Li Y, Sun H, Li D, Hou T (2013) Structural basis of the interactions between CXCR4 and CXCL12/SDF-1 revealed by theoretical approaches. Mol Biosyst 9:2107–2117
11. Kofuku Y, Yoshiura C, Ueda T et al (2009) Structural basis of the interaction between chemokine stromal cell-derived factor-1/CXCL12 and Its G-protein-coupled receptor CXCR4. J Biol Chem 284:35240–35250
12. Bilgin YM (2021) Use of plerixafor for stem cell mobilization in the setting of autologous and allogeneic stem cell transplantations: an update. J Blood Med 12:403–412
13. Bin CY, Le-Rademacher J, Brazauskas R et al (2019) Plerixafor alone for the mobilization and transplantation of HLA-matched sibling donor hematopoietic stem cells. Blood Adv 3:875–883
14. Kouroukis CT, Varela NP, Bredeson C, Kuruvilla J, Xenocostas A (2016) Plerixafor for autologous stem-cell mobilization and transplantation for patients in Ontario. Curr Oncol 23:e409–e430

15. Kymes SM, Pusic I, Lambert DL, Gregory M, Carson KR, DiPersio JF (2012) Economic evaluation of plerixafor for stem cell mobilization. Am J Manag Care 18:33–41
16. Alcázar-Valle M, Lugo-Cervantes E, Mojica L, Morales-Hernandez N, Reyes-Ramirez H, Enriquez-Vara JN, Garcia-Morales S (2020) Bioactive compounds, antioxidant activity, and antinutritional content of legumes: a comparison between four phaseolus species. Molecules 25:3528
17. Meenu M, Chen P, Mradula M, Chang SKC, Xu B (2023) New insights into chemical compositions and health-promoting effects of black beans (*Phaseolus vulgaris* L.). Food Front 4:1–20
18. Díaz-Batalla L, Widholm JM, Fahey GC, Castaño-Tostado E, Paredes-López O (2006) Chemical components with health implications in wild and cultivated Mexican common bean seeds (*Phaseolus vulgaris* L.). J Agric Food Chem 54:2045–2052
19. Ezzat SM, Abdel Rahman MF, Salama MM, Mahrous EA, El Bariary A (2022) Non-polar metabolites of green beans (*Phaseolus vulgaris* L.) potentiate the antidiabetic activity of mesenchymal stem cells in streptozotocin-induced diabetes in rats. J Food Biochem 46:1–14
20. Alcázar-Valle M, Lugo-Cervantes E, Mojica L, Morales-Hernández N, Reyes-Ramírez H, Enríquez-Vara JN, García-Morales S (2020) Bioactive compounds, antioxidant activity, and antinutritional content of legumes: a comparison between four phaseolus species. Molecules 25:3528
21. Lipinski CA (2004) Lead- and drug-like compounds: the rule-of-five revolution. Drug Discov Today 1:5
22. Syaban MFR, Faratisha IFD, Yunita KC, Erwan E, Kurniawan DB, Putra GFA (2022) Molecular docking and interaction analysis of propolis compounds against SARS-CoV-2 receptor. J Trop Life Sci 12:12
23. Lomize AL, Hage JM, Schnitzer K, Golobokov K, LaFaive MB, Forsyth AC, Pogozheva ID (2019) PerMM: a web tool and database for analysis of passive membrane permeability and translocation pathways of bioactive molecules. J Chem Inf Model 59:3094–3099
24. Mirdita M, Schütze K, Moriwaki Y, Heo L, Ovchinnikov S, Steinegger M (2022) ColabFold: making protein folding accessible to all. Nat Methods 19:679–682
25. Laskowski RA, Rullmannn JA, MacArthur MW, Kaptein R, Thornton JM (1996) AQUA and PROCHECK-NMR: programs for checking the quality of protein structures solved by NMR. J Biomol NMR 8:477–486
26. Smith EW, Liu Y, Getschman AE et al (2014) Structural analysis of a novel small molecule ligand bound to the CXCL12 chemokine. J Med Chem 57:9693–9699
27. Wu B, Chien EYT, Mol CD et al (2010) Structures of the CXCR4 chemokine receptor in complex with small molecule and cyclic peptide antagonists. Science 330:1066–1071
28. Syaban MFR, Erwan NE, Syamsuddin MRR, Zahra FA, Sabila FL (2022) Insilico study and analysis antibacterial activity of beta-glucan against beta-lactamase and protein binding penicillin-2A. Res J Pharm Technol 15:1948–1952
29. Rahman PA, Syaban MFR, Anoraga SG, Sabila FL (2022) Molecular docking analysis from *Bryophyllum pinnatum* compound as A COVID-19 cytokine storm therapy. Open Access Maced J Med Sci 10:779–784
30. Yueniwati Y, Syaban MFR, Erwan NE, Putra GFA, Krisnayana AD (2021) Molecular docking analysis of ficus religiosa active compound with anti-inflammatory activity by targeting tumour necrosis factor alpha and vascular endothelial growth factor receptor in diabetic wound healing. Open Access Maced J Med Sci 9:1031–1036
31. Yueniwati Y, Syaban MFR, Faratisha IFD, Yunita KC, Putra GFA, Kurniawan DB, Erwan NE (2021) Molecular docking approach of natural compound from herbal medicine in java against severe acute respiratory syndrome coronavirus-2 receptor. Open Access Maced J Med Sci 9:1181–1186
32. Syaban MFR, Erwan NE, Syamsuddin MRR, Zahra FA, Sabila FL (2021) Molecular docking approach of viscosin as antibacterial for methicillin-resistant *Staphylococcus aureus* via β-lactamase inhibitor mechanism. Clin Res J Intern Med 2:187–192
33. Meng EC, Goddard TD, Pettersen EF, Couch GS, Pearson ZJ, Morris JH, Ferrin TE (2023) UCSF ChimeraX: tools for structure building and analysis. Protein Sci 32:e4792
34. Bjelkmar P, Larsson P, Cuendet MA, Hess B, Lindahl E (2010) Implementation of the CHARMM force field in GROMACS: analysis of protein stability effects from correction maps, virtual interaction sites, and water models. J Chem Theory Comput 6:459–466
35. Sharma KP (2019) Tannin degradation by phytopathogen's tannase: a plant's defense perspective. Biocatal Agric Biotechnol 21:101342
36. Sudhakaran M, Sardesai S, Doseff AI (2019) Flavonoids: new frontier for immuno-regulation and breast cancer control. Antioxidants 8:103
37. Chávez-Mendoza C, Sánchez E (2017) Bioactive compounds from Mexican varieties of the common bean (*Phaseolus vulgaris*): implications for health. Molecules 22:1360
38. Benet LZ, Hosey CM, Ursu O, Oprea TI (2016) BDDCS, the rule of 5 and drugability. Adv Drug Deliv Rev 101:89–98
39. Cheng L, Wong H (2020) Food effects on oral drug absorption: application of physiologically-based pharmacokinetic modeling as a predictive tool. Pharmaceutics 12:672
40. Durán-Iturbide NA, Díaz-Eufracio BI, Medina-Franco JL (2020) In silico ADME/Tox profiling of natural products: a focus on BIOFACQUIM. ACS Omega 5:16076–16084
41. Baghel P, Roy A, Verma S, Satapathy T, Bahadur S (2020) Amelioration of lipophilic compounds in regards to bioavailability as self-emulsifying drug delivery system (SEDDS). Future J Pharm Sci 6:21
42. Boyd BJ, Bergström CAS, Vinarov Z et al (2019) Successful oral delivery of poorly water-soluble drugs both depends on the intraluminal behavior of drugs and of appropriate advanced drug delivery systems. Eur J Pharm Sci 137:104967
43. Bhalani DV, Nutan B, Kumar A, Singh Chandel AK (2022) Bioavailability enhancement techniques for poorly aqueous soluble drugs and therapeutics. Biomedicines 10:2055
44. Yuniwati Y, Syaban M, Anoraga S, Sabila F (2022) Molecular docking approach of *Bryophyllum pinnatum* compounds as atherosclerosis therapy by targeting adenosine monophosphate-activated protein kinase and inducible nitric oxide synthase. Acta Inform Med 30:91
45. Pernas S, Martin M, Kaufman PA et al (2018) Balixafortide plus eribulin in HER2-negative metastatic breast cancer: a phase 1, single-arm, dose-escalation trial. Lancet Oncol 19:812–824
46. Zhao R, Liu J, Li Z, Zhang W, Wang F, Zhang B (2022) Recent advances in CXCL12/CXCR4 antagonists and nano-based drug delivery systems for cancer therapy. Pharmaceutics 14:1541
47. Caspar B, Cocchiara P, Melet A, Van Emelen K, Van der Aa AA, Milligan G, Herbeuval J-P (2022) CXCR4 as a novel target in immunology: moving away from typical antagonists. Future Drug Discov 4:FDD77
48. Nugraha RYB, Faratisha IFD, Mardhiyyah K et al (2020) Antimalarial properties of isoquinoline derivative from *Streptomyces hygroscopicus* subsp. Hygroscopicus: an in silico approach. BioMed Res Int 2020:1–15
49. Uzzaman M, Chowdhury MK, Belal Hossen M (2019) Thermochemical, molecular docking and ADMET studies of aspirin metabolites. Front Drug Chem Clin Res 2:1–5
50. Syaban MFR, Rachman HA, Arrahman AD, Hudayana N, Purna J, Pratama FA (2021) Allium sativum as antimalaria agent via falciapin protease-2 inhibitor mechanism: molecular docking perspective. Clin Res J Internal Med 2:130
51. Kastritis PL, Bonvin AMJJ (2013) On the binding affinity of macromolecular interactions: daring to ask why proteins interact. J R Soc Interface 10:20120835
52. Challapa-Mamani MR, Tomás-Alvarado E, Espinoza-Baigorria A, León-Figueroa DA, Sah R, Rodriguez-Morales AJ, Barboza JJ (2023) Molecular docking and molecular dynamics simulations in related to *Leishmania donovani*: an update and literature review. Trop Med Infect Dis 8:457
53. Mohanty M, Mohanty PS (2023) Molecular docking in organic, inorganic, and hybrid systems: a tutorial review. Monatshefte Für Chem Chem Mon 154:683–707
54. Pantsar T, Poso A (2018) Binding affinity via docking: fact and fiction. Molecules 23:1899
55. Santos LHS, Ferreira RS, Caffarena ER (2019) Integrating molecular docking and molecular dynamics simulations. In: Azevedo de Jr WF (ed) Docking screens for drug discovery. Springer, New York, pp 13–34
56. Yueniwati Y, Syaban MFR, Kurniawan DB et al (2024) 7,8-Dihydroxyflavone functions as an antioxidant through the inhibition of Kelch-like ECH-associated protein 1: molecular docking and an *in vivo* approach in a rat model of ischemia-reperfusion brain injury. World Acad Sci J 6:1–14
57. Hospital A, Goñi JR, Orozco M, Gelpi JL (2015) Molecular dynamics simulations: advances and applications. Adv Appl Bioinf Chem 8:37–47

58. Villalvilla A, Gomez R, Roman-Blas JA, Largo R, Herrero-Beaumont G (2014) SDF-1 signaling: a promising target in rheumatic diseases. Expert Opin Ther Targets 18:1077–1087
59. Chen Y-B, Le-Rademacher J, Brazauskas R et al (2019) Plerixafor alone for the mobilization and transplantation of HLA-matched sibling donor hematopoietic stem cells. Blood Adv 3:875–883
60. Davatchi F, Sadeghi Abdollahi B, Mohyeddin M, Nikbin B (2016) Mesenchymal stem cell therapy for knee osteoarthritis: 5 years follow-up of three patients. Int J Rheum Dis 19:219–225
61. Luque-Campos N, Contreras-López RA, Jose Paredes-Martínez M et al (2019) Mesenchymal stem cells improve rheumatoid arthritis progression by controlling memory T cell response. Front Immunol 10:798
62. Dantara TWI, Syaban MFR et al (2021) Effect of *Bryophyllum pinnatum* leaves ethanol extract in TNF-α and TGF-β as candidate therapy of SLE in pristane-induced SLE BALB/c mice model. Res J Pharm Technol 14:1069–1072
63. Dantara TWI, Syaban MFR, et al. (2019) Efficacy and side effects studies of *Bryophyllum pinnatum* leaves ethanol extract in pristane-induced SLE BALB/c mice model. In: AIP Conference Proceedings, vol. 2108, (pp. 020016)
64. Duan L, Rao X, Sigdel KR (2019) Regulation of inflammation in autoimmune disease. J Immunol Res 1–2:2019
65. Santoso W, Putra G, Syaban M, Vadhana R, Khamid J, Maududi I, Sujuti H (2023) Integrated molecular docking, dynamic simulations and *in vivo* analysis of ethanol extract *Citrus sinensis* peel as an antioxidant and neurotrophic agent for ameliorating motor and cognitive functions in traumatic brain injury. World Acad Sci J 5:29
66. Ning Y, Wu Y, Zhou Q, Teng Y (2023) The effect of quercetin in the yishen tongluo jiedu recipe on the development of prostate cancer through the Akt1-related CXCL12/CXCR4 pathway. Comb Chem High Throughput Screen 27:863–876
67. Lotfi N, Yousefi Z, Golabi M et al (2023) The potential anti-cancer effects of quercetin on blood, prostate and lung cancers: an update. Front Immunol 14:1077531
68. Ye C, Zhang C, Huang H et al (2018) The natural compound myricetin effectively represses the malignant progression of prostate cancer by inhibiting PIM1 and disrupting the PIM1/CXCR4 interaction. Cell Physiol Biochem 48:1230–1244
69. Fonseca-Hernández D, Lugo-Cervantes EDC, Escobedo-Reyes A, Mojica L (2021) Black bean (*Phaseolus vulgaris* L.) polyphenolic extract exerts antioxidant and antiaging potential. Molecules 26(21):6716
70. Ferreira CD, Ziegler V, Lindemann IDS, Hoffmann JF, Vanier NL, Oliveira M (2018) Quality of black beans as a function of long-term storage and moldy development: chemical and functional properties of flour and isolated protein. Food Chem 246:473–480. https://doi.org/10.1016/j.foodchem.2017.11.118

Publisher's Note